

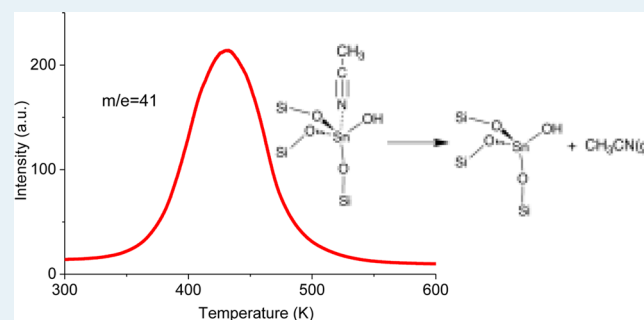
## Probing Lewis Acid Sites in Sn-Beta Zeolite

Sounak Roy,<sup>†,§</sup> Kevin Bakhmutsky,<sup>‡</sup> Eyas Mahmoud,<sup>†</sup> Raul F. Lobo,<sup>†</sup> and Raymond J. Gorte<sup>\*,†,‡</sup><sup>†</sup>Catalysis Center for Energy Innovation (CCEI), Department of Chemical and Biomolecular Engineering, University of Delaware, Newark, Delaware 19716, United States<sup>‡</sup>Department of Chemical & Biomolecular Engineering, University of Pennsylvania, Philadelphia, Pennsylvania 19104, United States

## Supporting Information

**ABSTRACT:** The adsorption properties of framework Sn sites in a siliceous zeolite beta were examined by comparing the adsorption of acetonitrile, diethyl ether, and 2-methyl-2-propanol on a Sn-Beta zeolite, a purely siliceous Beta zeolite, and a siliceous Beta zeolite with impregnated SnO<sub>2</sub>, using temperature-programmed desorption (TPD) and thermogravimetric analysis (TGA). Adsorption stoichiometries close to one molecule per framework Sn site were observed for each of the probe molecules. Although the 1:1 complexes with acetonitrile and diethyl ether decompose reversibly upon mild heating in vacuo, the 1:1 complex formed by 2-methyl-2-propanol underwent dehydration to butene and water over a very narrow temperature range centered at 410 K. FTIR spectra of acetonitrile-*d*<sub>3</sub> at a coverage of one molecule per site exhibit a  $\nu(\text{C}-\text{N})$  stretching frequency at 2312 cm<sup>-1</sup> that is not observed with nonframework Sn, providing a convenient method for characterizing the presence of framework Sn sites. Water interacts strongly enough with the Sn sites to prevent adsorption of acetonitrile.

**KEYWORDS:** Sn-Beta, temperature programmed desorption, Lewis catalysis, tin zeolites, Lewis acid base complexes



## INTRODUCTION

The highly siliceous zeolite beta, with framework-substituted Sn atoms, has generated much interest as a catalyst capable of carrying out important reactions in aqueous media. This material has demonstrated high selectivity and good stability for the catalytic oxidation of saturated and unsaturated ketones by hydrogen peroxide (the Baeyer–Villiger reaction),<sup>1</sup> the reduction of carbonyl compounds with secondary alcohols (the Meerwein–Ponndorf–Verley reaction),<sup>2</sup> the isomerization of glucose to fructose,<sup>3</sup> and the conversion of various pentoses and hexoses into methyl lactate.<sup>4</sup> In each of these reactions, the framework tin atoms act as Lewis-acid sites. The water tolerance, highly unusual for Lewis acids, is almost certainly due in part to the hydrophobic environment created by the siliceous cavities in the zeolite.

As with all zeolites, the structure of zeolite beta is formed from four-connected tetrahedral building units. These units are silica (SiO<sub>4/2</sub>) and alumina (AlO<sub>4/2</sub>)<sup>-</sup> in aluminosilicate zeolite beta but many other elements such as Sn, Ge, Zr, B, and others have been incorporated into the zeolite beta framework. The pores in zeolite beta are relatively large (12-membered ring, 0.73 nm in diameter) and intersect to form a three-dimensional pore system allowing rapid diffusion of reactants and products.<sup>5</sup> In Al-containing zeolites, Brønsted-acid sites are generated when the charge associated with AlO<sub>4</sub><sup>-</sup> tetrahedra is balanced by a hydrogen ion. However, isomorphous, framework substitution of Sn<sup>IV</sup> for Al results in Lewis-acid sites. Based

on FTIR studies of acetonitrile adsorption and theoretical calculations, it has been reported that there are two types of framework Sn sites, one consisting of a fully framework Sn (closed sites) and the other formed by hydrolysis of one of the Sn–O–Si bridges to generate a (–Si–O–)<sub>3</sub>Sn–OH site (open sites).<sup>6</sup> It has been argued that the open sites are more active catalytically. These same two types of framework sites have also been reported for Ti substitution in materials having the ZSM-5 structure<sup>7</sup> (i.e., TS-1).

An important advance in the characterization of Brønsted sites associated with framework Al in high-silica zeolites came from the observation that many adsorbates form stoichiometric complexes with the acid sites.<sup>8–10</sup> Through spectroscopic studies of the reactivity of various complexes and measurements of the adsorption energies of a wide range of adsorbates, semiquantitative models were developed that are useful for understanding reactions at the acid sites and for predicting the chemistry of other molecules.<sup>11</sup> In the present study, we determine whether similar stoichiometric complexes could form at the Lewis sites associated with framework Sn. Because TPD-TGA (Temperature-Programmed Desorption, Thermogravimetric Analysis) measurements provided the clearest evidence for stoichiometric complexes in the case of Al-containing

Received: September 13, 2012

Revised: February 17, 2013

Published: February 20, 2013

zeolites, this has been used as the primary technique here. For probe molecules, we chose a simple alcohol (2-methyl-2-propanol) and a simple ether (diethylether) because of the importance of framework Sn sites in converting oxygenated hydrocarbons. Acetonitrile has already been shown to be a good probe of Lewis sites;<sup>6</sup> by matching TPD-TGA and FTIR measurements, the effect of acetonitrile coverage on the vibrational spectra could be determined.

We show here that adsorption complexes are formed at framework Sn sites and that adsorption on nonframework Sn sites exhibits different characteristics. Although we are unable to distinguish “open” and “closed” framework sites, matching of TPD-TGA and FTIR data demonstrated that there is an effect on the vibrational spectrum of acetonitrile when there is more than one molecule at the site, so that characterization of the sites by FTIR requires careful dosing of the sample. Our results also demonstrate that Sn-Beta has potential for gas phase catalytic reactions in addition to the liquid phase reactions for which it has been exclusively investigated so far.

## ■ EXPERIMENTAL METHODS

**Materials Synthesis.** The siliceous form of zeolite beta (referred to in this paper as Si-Beta) was prepared following the protocol reported by Cambor et al.<sup>12</sup> First, 8.08 g of tetraethylammonium hydroxide (TEAOH, 40 wt % Sigma Aldrich) and 1.44 g of deionized (DI) water were mixed at room temperature in a covered polypropylene container. To this, 8.47 g of tetraethylorthosilicate (TEOS, Sigma Aldrich, 98%) is added, and the mixture then stirred at room temperature for 6.5 h. Ethanol formed by hydrolysis was allowed to evaporate at room temperature and was replaced with DI water. To this solution, 0.915 g of HF (48 wt %, Sigma Aldrich, fresh) was added, resulting in a final solution composition of 0.54 TEAOH:0.54 HF: SiO<sub>2</sub>:7.25 H<sub>2</sub>O. After transferring the mixture to a Teflon-lined, stainless steel autoclave (Parr), it was heated in a convection oven to 413 K, with rotation (~40 rpm). After 14 days, the autoclave was quenched, the contents filtered, and the solid washed with deionized water. The solid was calcined in air at 830 K for 8 h, using a temperature ramp of 5 K/min to get from room temperature to 830 K.

Zeolite beta with framework Sn (Sn-Beta) was prepared according to the procedure described by Corma and Valencia.<sup>2</sup> First, 13.6 g of TEOS (Sigma Aldrich, 98%) were hydrolyzed in 13.01 g of TEAOH (40 wt %, Sigma Aldrich) with stirring at room temperature. To this solution, 0.1840 g of SnCl<sub>4</sub>·5H<sub>2</sub>O (Strem Chemicals, 98% reagent grade) in 0.92 g of DI water were added, after which the mixture was again stirred at room temperature until the solution had decreased in weight by 12 g because of ethanol evaporation. To the resulting clear solution, 1.47 g of HF (48 wt %) were added, causing the formation of a thick paste. Next, 0.152 g of calcined, siliceous zeolite Si-Beta in 0.73 g of DI water was added as seed crystals. The final gel composition was as follows: 1.0 SiO<sub>2</sub>: 0.0083 SnO<sub>2</sub>: 0.54 TEAOH: 7.5 H<sub>2</sub>O: 0.54 HF. The crystallization was carried out in rotating, Teflon-lined, stainless-steel autoclaves at 413 K for 14 days. The solid produced by this process was then calcined in air using a heating ramp of 3 K/min to 853 K and held at this temperature for an additional 3 h.

To determine the effect of nonframework Sn, a sample was prepared by simple impregnation of Sn into Si-Beta (EF-Sn-Beta). A solution made from 0.03 g of SnCl<sub>4</sub>·5 H<sub>2</sub>O (Strem Chemicals, 98% reagent grade) dissolved in 0.125 mL of

HPLC-grade methanol (Fischer Scientific, 99.9%) was added to the calcined Si-Beta zeolite with stirring and the mixture was allowed to dry overnight at room temperature. The resulting catalyst was heated to 873 K using a heating rate of 5 K/min and then held at 873 K for 5 h.<sup>13</sup> The composition of the sample corresponded to a Si:Sn ratio of 100.

**Analytical Methods.** <sup>119</sup>Sn MAS NMR experiments were recorded on a Bruker AVIII-500 solid-state NMR spectrometer, operating at a Larmor frequency of 186.5 MHz for <sup>119</sup>Sn. A 4 mm HX MAS probe was used. The magic angle spinning rate was set to 12,000 ± 2 Hz for all measurements. The <sup>119</sup>Sn 90 degree pulse was calibrated to be 6.0 μs using saturated SnCl<sub>4</sub> solution. Single pulse experiment with a recycle delay of 50 s was used with the number of scans ranging from 1024 to 4320, depending on the signal-to-noise ratio of spectrum. The spectra were referenced externally to a peak of <sup>119</sup>Sn spectrum of SnO<sub>2</sub> at -604.3 ppm.<sup>14</sup>

The samples were analyzed using a UV/vis spectrometer (Jasco V-550) equipped with a diffuse-reflectance cell<sup>15</sup> because earlier work has demonstrated the effectiveness of this technique for the characterization of framework Sn in siliceous zeolites.<sup>3</sup> The spectra were transformed by the Kubelka–Munk function:

$$F(R) = \frac{(1 - R)^2}{2R} = K/S \quad ([1])$$

where  $R$  indicates the ratio of the diffuse reflectance determined on the sample relative to that of a reference material (barium sulfate),  $K$  is the absorption coefficient, and  $S$  the scattering coefficient of the powder. The samples were analyzed after calcination, using the same baseline in each case.

X-ray powder diffraction (XRD) patterns were recorded on a Phillips X'Pert X-ray diffractometer using Cu K $\alpha$  radiation. A Si sample was used as an internal standard for determining precise peak positions. Unit cell dimensions were calculated using the program UNITCELL,<sup>16</sup> indexing the powder pattern using only well-defined reflections according to the tetragonal unit cell of the end-member polytype A (BEA\*).

The micropore volumes of samples were determined using nitrogen adsorption isotherms at 77 K measured using a Micromeritics ASAP 2020 instrument. All samples were degassed for 8 h under vacuum at 300 °C before adsorption measurements. The micropore volumes and surface areas of Beta zeolites were determined using the t-plot method.

Temperature Programmed Desorption (TPD) and Thermogravimetric Analysis (TGA) experiments were carried out using a CAHN 1000 microbalance mounted within a high vacuum chamber, as described elsewhere.<sup>17</sup> The base pressure of the system was 1 × 10<sup>-8</sup> Torr. During TPD-TGA measurements, the sample weight could be recorded continuously using the microbalance and the desorbing species monitored using a UTI quadrupole mass spectrometer. The peaks intensities at selected  $m/e$  from the mass spectra are reported here in arbitrary units (a.u.). The sample temperature was measured with a thermocouple placed near the sample, and the heating rate during desorption was maintained at 10 K/min by a temperature controller. Unless otherwise noted, the samples were heated in vacuo to 773 K, then cooled in vacuo, prior to exposing them to the vapors of the adsorbate of interest. The solid samples were exposed to the probe molecules (diethyl ether, acetonitrile, and 2-methyl-2-propanol) at room temperature using 3 Torr of vapor until there was no further uptake. The system was then evacuated for 1 h

before beginning the TPD-TGA experiment. In experiments to examine the effect of adsorbed water, the samples were exposed to 3 Torr of water vapor at room temperature, then evacuated for 1 h prior to dosing the samples with the adsorbate of interest.

FTIR spectra were collected on a Mattson Galaxy FTIR with a diffuse-reflectance attachment (Collector II) purchased from Spectra-Tech Inc. Spectra were collected at  $2\text{ cm}^{-1}$  resolution. The samples were initially heated to 773 K in flowing He to remove any water. After cooling the samples to room temperature, acetonitrile- $d_3$  vapors were exposed to the sample, with the excess acetonitrile then flushed from the solid using flowing He at  $1\text{ cm}^3/\text{s}$ . FTIR spectra were collected also on hydrated samples.

Chemical composition was determined using inductively coupled plasma-optical emission spectroscopy (ICP-OES) measured by Galbraith Laboratories (Tennessee). This analysis showed that the compositions of the Sn-Beta and EF-Sn-Beta samples are very similar, with Si/Sn ratios of 118 and 106, respectively. On dehydrated samples, these Si/Sn ratios correspond to  $140\text{ }\mu\text{mol Sn/g}$  and  $150\text{ }\mu\text{mol Sn/g}$ , respectively.

## RESULTS

**Materials Characterization.** Previous reports have indicated that incorporation of Sn into the framework of zeolite beta can be difficult; therefore, the samples were first characterized by a number of techniques before examining the adsorption properties. XRD measurements gave diffraction patterns for each of the samples that were consistent with the structure of zeolite beta, with no impurity phases and undetectable amounts of amorphous material (see the Supporting Information section). Because the structure of zeolite beta is disordered (an intergrowth of two polytypes), determination of accurate unit cell dimensions required precise measurements and analysis to conclusively show that there is an increase in the unit cell size upon framework substitution of Si for the much larger Sn cations. Table 1 shows that, within

**Table 1. Unit Cell Dimensions of Si-Beta, Sn-Beta, and EF-Sn-Beta**

sample	$a = b$ (Å)	$c$ (Å)	unit cell volume (Å <sup>3</sup> )
Si-Beta	$12.469 \pm 0.004$	$26.21750 \pm 26.21750$	$4076 \pm 2.3$
EF-Sn-Beta	$12.463 \pm 0.004$	$26.21 \pm 0.01$	$4073 \pm 2.3$
Sn-Beta	$12.474 \pm 0.004$	$26.25 \pm 0.01$	$4084 \pm 2.3$

experimental error, the unit cell volumes for the Si-Beta and EF-Sn-Beta samples are the same, while the unit cell volume for the Sn-Beta sample is slightly larger. These results also indicate that simple impregnation of Sn salts into a siliceous Beta zeolite does not lead to framework substitution and that at least some of the Sn was incorporated into the framework of the Sn-Beta sample.

Surface area measurements using nitrogen adsorption isotherms (Table 2) show that Sn-Beta and Si-Beta have high microporous volumes ( $\sim 0.20\text{ cm}^3/\text{g}$ ) characteristic of zeolite beta samples of good quality. This table also shows that the microporous volume of Si-Beta decreases substantially upon impregnation with  $\text{SnO}_2$ , from  $0.21$  to  $0.14\text{ cm}^3/\text{g}$ . This decrease in volume indicates that a fraction of the tin precursor has penetrated into the zeolite micropores, likely forming small clusters of tin oxide inside the zeolite pores (see below). Note,

**Table 2. Textural Properties of Si-Beta, Sn-Beta, and EF-Sn-Beta**

sample	microporous <sup>a</sup> volume ( $\text{cm}^3\text{ g}^{-1}$ )	external surface area <sup>a</sup> ( $\text{m}^2\text{ g}^{-1}$ )	specific surface area <sup>a</sup> ( $\text{m}^2\text{ g}^{-1}$ )
Si-Beta	0.21	64.06	384
EF-Sn-Beta	0.14	99.47	302
Sn-Beta	0.19	93.15	411

<sup>a</sup>Determined using the t-plot method.

however, that this result does not exclude the possibility of  $\text{SnO}_2$  formation outside the zeolite micropores.

**<sup>119</sup>Sn MAS NMR Spectroscopy.** <sup>119</sup>Sn MAS NMR spectra collected from Sn-Beta and EF-Sn-Beta show clear differences between the samples (see Supporting Information, Figure S2). The Sn-Beta sample shows (weak) resonances centered at  $-688\text{ ppm}$  and a shoulder at higher fields that have been assigned to hydrated framework Sn sites. This spectrum is very similar to the spectra of Sn-Beta samples prepared by the Davis' group<sup>14</sup> for samples containing Sn in the framework and showing good catalytic activity for glucose isomerization reactions. Within the limits of the signal/noise ratio of the spectrum (Supporting Information, Figure S2 a) there is no evidence of a signal at  $\sim -604\text{ ppm}$  that would be expected for octahedral Sn in bulk  $\text{SnO}_2$ . On the other hand, the <sup>119</sup>Sn MAS NMR spectrum of EF-Sn-Beta (Supporting Information, Figure S2b) shows only a resonance centered near  $-604\text{ ppm}$  consistent with extra-framework Sn in Si-Beta.<sup>14</sup> Supporting Information, Figure S2 also shows the <sup>119</sup>Sn MAS NMR spectrum of crystalline  $\text{SnO}_2$  that clearly only displays a sharp signal at  $-604\text{ ppm}$  (and the associated spinning side bands) because of octahedral Sn in  $\text{SnO}_2$ . These spectra confirm that the sample of Sn-Beta contains only framework tin within the limits of the resolution of the technique.

**DRUV/vis Spectroscopy.** The Diffuse Reflectance UV/vis spectra for the three samples (Figures 1a and b) support the findings from <sup>119</sup>Sn MAS NMR spectroscopy. The Si-Beta sample shows only very weak and broad absorption features, while the Sn-Beta sample shows a peak centered at  $203\text{ nm}$  which has been assigned to tetrahedrally coordinated Sn.<sup>14</sup> The DRUV spectrum of EF-Sn-Beta shows a broad feature centered around  $248\text{ nm}$  which has been assigned to  $\text{SnO}_2$  species in Si-Beta.<sup>14</sup> Figure 1b depicts the DRUV spectrum in Kubelka–Munk units. (It is recommended to report DRUV spectra in these units as the Kubelka–Munk function is the counterpart of the absorbance function and relates intensities directly to concentration).<sup>15</sup> The Sn-Beta sample exhibits a well-defined absorption edge starting at  $\sim 300\text{ nm}$ . The absorption feature in the UV–vis spectrum has been assigned to an electronic transition on isolated  $\text{Sn}^{\text{IV}}$  species bonded to the zeolite framework via oxygen linkages. The EF-Sn-Beta sample also exhibits an absorption edge in the UV–vis spectrum, but the edge clearly starts at lower energy than for Sn-Beta. This figure and Supporting Information, Figure S3 show more clearly that there is a progression in energy of absorption in the order  $\text{SnO}_2 < \text{EF-Sn-Beta} < \text{Sn-Beta}$ .

There is a relation between the absorption edge energy and the domain size, so that clustering of  $\text{SnO}_2$  is observed as a shift in the absorption-edge energy. Therefore, the energies for our samples were calculated from the intercept of a straight line fitted through the low energy rise in the graphs of  $[F(R_\infty)h\nu]^2$  vs  $h\nu$ .<sup>3,19</sup> The absorption-edge energies for Sn-Beta, EF-Sn-Beta, and Sn(IV) oxide were determined to be  $4.38\text{ eV}$ ,  $3.89$



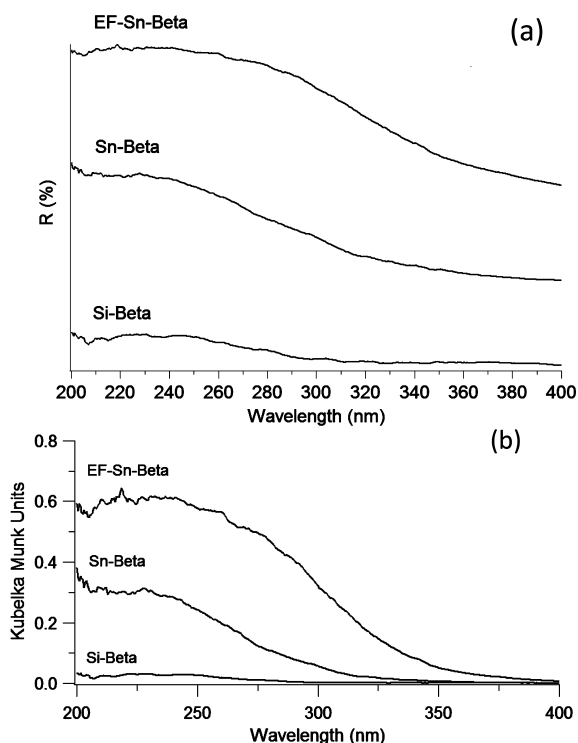


**Figure 1.** Reflectance UV/vis spectra of Si-Beta, Sn-Beta, and EF-Sn-Beta.

eV, and 3.80 eV, respectively. Pang et al.<sup>20</sup> have investigated the optical properties of SnO<sub>2</sub> particles of different sizes and have shown that particles of approximately 3.5 nm in diameter have an absorption edge around 3.98 eV. Taking the isolated tin species in Sn-Beta as the limit of the smallest particle size attainable, it is clear that the EF-Sn-Beta sample contains molecular clusters or aggregates of tin oxide/hydroxide. The energy of the absorption edge shows that the largest particles present in our samples are  $\sim 4.1$  nm in diameter. These SnO<sub>2</sub> nanoparticles are in fact too large to fit in the pores of the zeolites and consequently must be outside the zeolite crystals. Yet, the adsorption studies indicate that SnO<sub>2</sub> species reside in part in the pores of the zeolite because of the lower microporous volume of these samples. It is possible then that SnO<sub>2</sub> particles are present inside and outside the relevant microcrystals with the UV/vis spectroscopy dominated by the properties of the larger particles ( $\sim 4.1$  nm) and other properties affected by the presence of SnO<sub>2</sub> clusters in the zeolite micropores.

In summary, the characterization data show that Si-Beta, Sn-Beta, and EF-Sn-Beta have all the same overall structure, show that Si-Beta contains no active sites, and that the tin species in Sn-Beta are molecularly dispersed. The data also show that EF-Sn-Beta contains tin in the pores and in the crystal exterior giving rise to a large distribution of active sites.

**Adsorption Properties. Acetonitrile.** A previous report has shown that FTIR spectroscopy of adsorbed acetonitrile-*d*<sub>3</sub> is useful for characterization of the Lewis-acid sites in Sn-Beta.<sup>6</sup> Therefore, the three zeolite samples, Sn-Beta, EF-Sn-Beta, and Si-Beta, were examined using this probe molecule. TPD-TGA results for Si-Beta and Sn-Beta are shown in Figure 2a and results for EF-Sn-Beta in Figure 2b. Following exposure to 3 Torr of acetonitrile and evacuation for 1 h, the Si-Beta exhibited a weight change corresponding to an acetonitrile coverage of 40

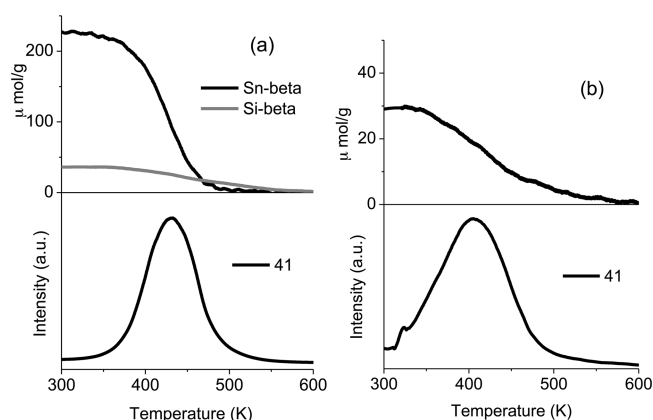


**Figure 2.** (a) TPD (lower curve) and TGA (upper curve) traces for acetonitrile from Sn-Beta, and Si-Beta. (b) TPD (lower curve) and TGA (upper curve) traces for acetonitrile from EF-Sn-Beta.

$\mu\text{mol/g}$ . This small coverage may be associated with adsorption at defect sites, possibly at the nested-silanol clusters that occur when there is a Si vacancy in the lattice.<sup>21</sup> In contrast, approximately 220  $\mu\text{mol/g}$  of acetonitrile remained on the Sn-Beta sample, a coverage that is in excess of the Sn concentration of the sample, 140  $\mu\text{mol/g}$ . While some of the excess acetonitrile may be associated with defects, it is likely that there is an affinity for more than one molecule on a single Sn cation because of the large size of the Sn cations. Indeed, adsorption above one molecule per site has been observed for CO on the cation sites of K- and Cs-exchanged ZSM-5.<sup>22</sup> In that example, the adsorption stoichiometry increased with the cation size, as expected; but the energy of adsorption of the second CO molecule was lower than that of the first. A weaker attraction between the second acetonitrile molecule and the Sn cations may explain the results for acetonitrile. Finally, additional evidence that two molecules can interact with a site comes from recent <sup>119</sup>Sn MAS NMR studies of Sn-Beta, which showed that the hydrated sample contains only octahedral tin requiring the binding of *two* water molecules to the Sn cation.<sup>18</sup>

The TPD-TGA results for acetonitrile on EF-Sn-Beta, reported in Figure 2b, are clearly different from the results found on Sn-Beta. Indeed, the acetonitrile coverage after evacuation for 1 h was only 30  $\mu\text{mol/g}$ , a value less than that measured on Si-Beta which was used in the preparation of the EF-Sn-Beta. This result suggests that the acetonitrile has either not adsorbed on the extra-framework Sn or is removed upon evacuation.

FTIR spectra of acetonitrile-*d*<sub>3</sub> in Sn-Beta and EF-Sn-Beta are given in Figures 3a and 3b, respectively. Although the zeolite sample size in the FTIR measurements was similar to that used in TPD-TGA, the removal of weakly held adsorbates by flowing dry He in the FTIR experiments is significantly less effective than the high vacuum used in TPD-TGA, so that acetonitrile coverages are much higher here. Spectra of the Sn-Beta sample at room temperature during acetonitrile-*d*<sub>3</sub> exposure, spectrum (i), shows two  $\nu(\text{C-N})$  stretches, centered at 2275  $\text{cm}^{-1}$  and 2310  $\text{cm}^{-1}$ . As excess acetonitrile is removed from the Sn-Beta sample by mild heating and continued flushing with He, the 2275  $\text{cm}^{-1}$  feature decreases, while the feature at 2310  $\text{cm}^{-1}$  narrows and shifts to 2312  $\text{cm}^{-1}$ . For the EF-Sn-Beta sample, only one  $\nu(\text{C-N})$  peak is observed at 2263  $\text{cm}^{-1}$ , with a shoulder extending toward higher wavenumbers.

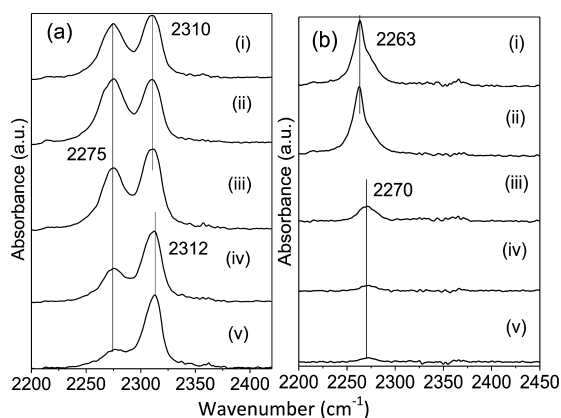


**Figure 3.** (a) FTIR spectra of Sn-Beta in (i) He flow with CD<sub>3</sub>CN vapor at RT; (ii) in pure He flow at RT immediately removing CD<sub>3</sub>CN vapor; (iii) in He flow after heating to 373 K for 1 min; (iv) in He flow after heating to 373 K for 2 min; (v) in He flow after heating to 373 K for 3 min. (b) FTIR of EF-Sn-Beta in (i) He flow with CD<sub>3</sub>CN vapor at RT; (ii) in pure He flow at room temperature (RT) immediately after removing CD<sub>3</sub>CN vapor; (iii) in He flow after heating to 373 K for 1 min; (iv) in He flow after heating to 373 K for 2 min; (v) in He flow after heating to 373 K for 3 min.

With He flushing, only a feature centered at 2270 cm<sup>-1</sup> remains and even this feature is removed with relative ease. Most notably, there is no evidence for a feature near 2310 cm<sup>-1</sup>.

In Figure 3, the spectral features at 2263 and 2275 cm<sup>-1</sup> are likely associated with molecules that are not interacting with the Sn sites. Indeed, a peak at 2275 cm<sup>-1</sup> was reported in adsorption studies on acidic H-ZSM-5 when the acetonitrile coverage was in large excess over the acid site density.<sup>23</sup> Because the position of the  $\nu(\text{C-N})$  changes with solvent,<sup>24</sup> the shifts with coverage may simply be related to changes in packing of the molecules within the pores. The features near 2310 cm<sup>-1</sup> are clearly associated with framework Sn sites, in agreement with a previous report.<sup>6</sup> While that report suggested that small shifts in that peak may be due to “open” and “closed” sites, it is also possible that the shifts are associated with “solvent” effects due to the presence or absence of additional acetonitrile molecules in the vicinity. Whether or not the FTIR spectra are able to distinguish different types of framework Sn remains to be confirmed; however, the  $\nu(\text{C-N})$  frequencies certainly are able to distinguish framework and nonframework tin.

**2-Methyl-2-Propanol and Diethyl Ether.** One of the most interesting applications for Sn-Beta is the conversion of glucose to fructose, for which the zeolite activates intramolecular hydride transfer between two adjacent C–O bonds.<sup>3,25</sup> Therefore, to probe how the framework Sn sites interact with ether and alcohol functional groups, we examined the adsorption of diethyl ether and 2-methyl-2-propanol. Figure 4a shows TPD-TGA results for diethyl ether in Sn-Beta and Si-Beta after exposure to 3 Torr of vapor, followed by evacuation for 1 h. The TGA data for Si-Beta indicate that all of the diethyl ether is removed by evacuation, while ~170  $\mu\text{mol/g}$ , a coverage that is very close to the framework Sn concentration, remains in the Sn-Beta sample. The diethyl ether desorbs intact as a narrow feature at 400 K. Interestingly, the TPD-TGA data for the EF-Sn-Beta sample, Figure 4b, reveals that there is some interaction of the ether with the nonframework Sn. The coverage after evacuation, ~90  $\mu\text{mol/g}$ , is lower than the Sn concentration, but much higher than that observed on the Si-

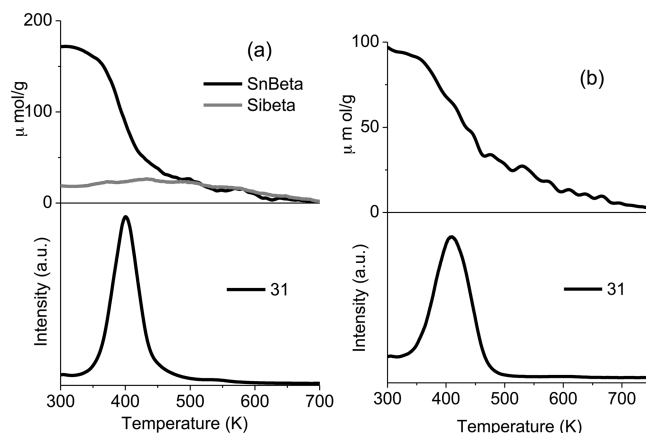


**Figure 4.** (a) TPD (lower curve) and TGA (upper curve) traces for diethyl ether from Sn-Beta and Si-Beta. (b) TPD (lower curve) and TGA (upper curve) traces for diethyl ether from EF-Sn-Beta.

Beta sample. Although the peak temperature is similar to that found with the Sn-Beta, the peak is broader with EF-Sn-Beta, suggesting that there are a range of adsorption environments. Because desorption from porous materials is coupled with diffusion and readsorption,<sup>26</sup> caution must be used in the interpretation of peak temperatures and peak width.

The TPD-TGA results following exposure to 3 Torr of 2-methyl-2-propanol and 1-h evacuation on each of the three samples is reported in Figure 5. Figure 5a was obtained from the Si-Beta sample: approximately 130  $\mu\text{mol/g}$  of the alcohol remained in the sample prior to heating, but all of the alcohol desorbed intact (The alcohol has peaks at  $m/e = 56$  and  $59$ ) in a broad feature centered at 420 K. From earlier studies in siliceous zeolites,<sup>10</sup> it is known that alcohols form relatively strong hydrogen bonds with defect sites and with other adsorbed alcohols. Since there can be a clustering of more than one molecule at a site, the amount of alcohol remaining in the sample following evacuation is likely much larger than the defect site concentration of this sample.

Results for the Sn-Beta sample in Figure 5b are more interesting. The coverage after evacuation is ~380  $\mu\text{mol/g}$ , well over twice the Sn concentration, suggesting that there is clustering of hydrogen-bonded molecules at the Sn sites. More than half of these molecules desorbed intact as 2-methyl-2-propanol, but an amount that is close to the Sn concentration desorbed as butene ( $m/e = 56$ ) and water ( $m/e = 18$ ). (Note that 2-methyl-2-propanol also has a peak at  $m/e = 18$  in its fragmentation pattern, so that the leading edge of the TPD curve for  $m/e = 18$  is due to unreacted alcohol.) The reaction feature for butene is very narrow, with a peak temperature of 410 K and a width at half-maximum of only 35 K, close to what would be expected for a unimolecular reaction of identical molecules with a normal pre-exponential factor. Since butene desorption is likely limited by the reaction of the alcohol, the narrow desorption peak suggests that the Sn sites are nearly identical.<sup>17</sup> Using the Redhead equation and a normal pre-exponential of  $10^{13} \text{ s}^{-1}$ , the activation energy for reaction of 2-methyl-2-propanol is 117 kJ/mol.

The TPD-TGA results for 2-methyl-2-propanol on EF-Sn-Beta in Figure 5c are qualitatively similar to those for Sn-Beta. The initial coverage is almost the same, and half of the alcohol again reacts to form butene and water. This indicates that the extra-framework Sn is accessible for adsorption and does have Lewis acidic properties. However, on the EF-Sn-Beta the

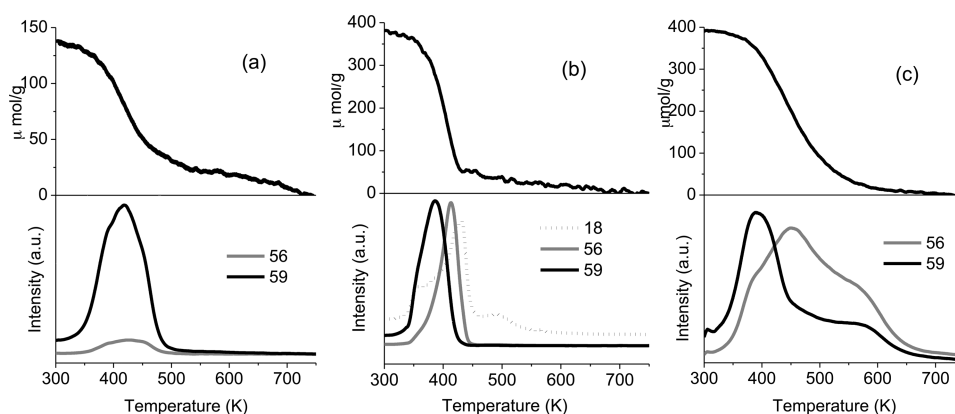


**Figure 5.** TPD (lower curves) and TGA (upper curves) traces for *tert*-butanol from (a) Si-Beta, (b) Sn-Beta, (c) EF-Sn-Beta. Species in the mass spectra were identified by noting that *tert*-butanol has peaks at  $m/e = 18, 56,$  and  $59$ , while butene has a peak at only  $m/e = 56$ .

desorption features are very broad, extending from below 400 K to above 600 K. Most of the dehydration reaction occurs at temperatures well above the 410 K peak temperature found with Sn-Beta. Finally, unreacted alcohol leaves the sample over the entire temperature range, implying that the alcohol molecules may bind with the extra-framework Sn but are much less reactive at those sites.

**Coadsorption of  $H_2O$ .** One of the most interesting aspects of reactions on Sn-Beta is that Lewis-acid reactions can occur in the presence of water. To determine whether water had any effect on adsorption, we performed TPD-TGA measurements with acetonitrile and with 2-methyl-2-propanol after first exposing the sample to 3 Torr of  $H_2O$  followed by 1-h evacuation. In the presence of 3 Torr  $H_2O$  vapor, the sample weight change was 0.0105 g  $H_2O/g$  zeolite, or 580  $\mu\text{mol/g}$ . This is well over two molecules per Sn atom and sufficient to explain the tetrahedral-to-octahedral change in the coordination geometry that has been reported for the site based on NMR spectroscopy.<sup>18</sup> After 1-h evacuation, the weight change was only 0.0030 g  $H_2O/g$  zeolite (170  $\mu\text{mol/g}$ ) or just over one molecule per Sn site. There is significant uncertainty in this measurement because of the low molecular weight of water; however, the water coverage after evacuation was certainly no greater than two molecules per site after evacuation. After this pretreatment, TPD-TGA measurements with the alcohol and the nitrile were carried out using the same procedures as in Figures 2 and 5.

Preadsorbed water had no effect on the data obtained for 2-methyl-2-propanol, and the TPD-TGA results were identical to those shown in Figure 5b. Adsorbed water was simply displaced by the alcohol. On the other hand, preadsorbed water completely blocked adsorption of acetonitrile. After exposure to 3 Torr of acetonitrile and evacuation for 1 h, all of the acetonitrile was removed in the hydrated sample. Since acetonitrile was present in large excess over water during the exposure, the fact that acetonitrile was unable to displace water implies that it interacts with the Sn sites much more weakly than does water. While water may not block Sn sites from reaction of molecules with alcohol functional groups, there is an affinity of the Sn sites for water.

The effect of preadsorbed water on the acetonitrile adsorption is shown by FTIR measurements in Figure 6. In this experiment, the Sn-Beta sample was exposed to water vapor at room temperature, then flushed with dry He for 1 h before exposing it to acetonitrile- $d_3$  vapor. Even with the large

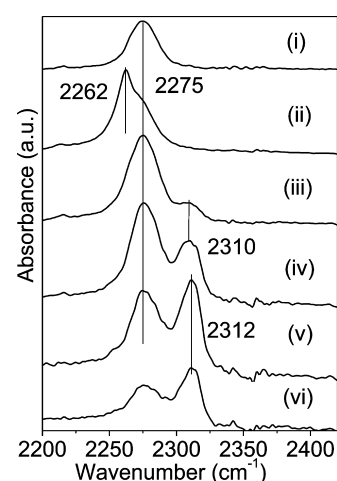


**Figure 6.** FTIR spectra obtained on Sn-Beta after exposure to water vapor at room temperature, followed by flushing with dry He. Spectra were obtained in (i) He flow in the presence of  $CD_3CN$  vapor at RT; (ii) in pure He flow at RT immediately after removing  $CD_3CN$  vapor; (iii) in He flow after heating to 373 K for 1 min; (iv) in He flow after heating to 373 K for 2 min; (v) in He flow after heating to 373 K for 3 min; (vi) in He flow after heating to 373 K for 4 min.

excess of acetonitrile present in the sample during exposure, the only  $\nu(C-N)$  stretch observed in the spectrum is at 2275  $\text{cm}^{-1}$ . Upon flushing with dry He, this peak decreases in intensity and a feature at 2262  $\text{cm}^{-1}$  appears, which is similar to that observed on EF-Sn-Beta in Figure 3. With mild heating to 373 K and continued He flow, the peak at 2310  $\text{cm}^{-1}$  begins to appear and grow at the expense of the lower frequency feature. We suggest that there is sufficient acetonitrile vapor still present in the IR cell following this mild heating so that molecules can adsorb on the Sn sites as the water desorbs. This result confirms that water interacts with the Sn sites to prevent acetonitrile adsorption.

## DISCUSSION

Sn-Beta is an intriguing catalytic material. Its ability to carry out Lewis-acid reactions of organic molecules in aqueous environments opens up important practical possibilities, particularly for the processing of biomass. The results we have reported here are useful in understanding and characterizing the catalytic sites.

First, the FTIR studies confirm reports that acetonitrile-*d*<sub>3</sub> can be used for characterizing framework Sn sites. The spectra reported here demonstrate that there is a clear distinction between framework and nonframework Sn as determined by the  $\nu(\text{C}-\text{N})$  stretching frequency. This difference cannot be explained by the argument that nonframework Sn is inaccessible to acetonitrile adsorption, since both framework and nonframework Sn sites were able to dehydrate 2-methyl-2-propanol. The FTIR observations are important in providing a simple, widely available method for confirming the quality of Sn-containing zeolites. However, our data do not support the idea that the vibrational spectra are able to distinguish between different types of framework Sn based on FTIR frequencies.

Second, the TPD-TGA results for all three probe molecules examined in this work demonstrate that the framework Sn sites provide a unique catalytic environment. The identification of adsorption states with a coverage close to the amount of framework Sn in the Sn-Beta sample demonstrates that Sn-Beta has discrete sites for molecules to interact with. The dehydration of 2-methyl-2-propanol to butene and water in TPD-TGA measurements indicates that the Sn sites are catalytically active (although here the reaction is stoichiometric, not catalytic). Even though nonframework SnO<sub>2</sub> is also able to catalyze the dehydration of 2-methyl-2-propanol, the fact that dehydration occurs at lower temperatures on framework Sn suggests that the framework Sn is a better catalytic site. Furthermore, the sharpness of the dehydration peak on Sn-Beta suggests that all framework Sn sites have very similar catalytic properties.

Finally, it is interesting that water is so effective in preventing the adsorption of acetonitrile, but not of 2-methyl-2-propanol, on framework Sn sites. This could have practical implications in understanding the effect of solvents on catalytic properties. For example, activation of nitrile groups by the Lewis sites associated with framework Sn will not be possible in aqueous solutions but may be possible with other solvents. From a theoretical standpoint, the observation that a coverage of only one or two water molecules per site can block adsorption of acetonitrile suggests that the water molecules may be modifying the Sn sites, not just blocking them. For example, if simple adsorption of water converted fully framework Sn (closed sites) into open sites ( $-\text{Si}-\text{O}-$ )<sub>3</sub>Sn-OH site (open sites),<sup>6,7</sup> there would be mechanistic implications for understanding the site geometry.

Obviously, additional work will be needed to fully understand the nature of the Lewis-acid sites associated with framework Sn in siliceous zeolites. We believe that well-defined adsorption complexes provide a useful tool for characterizing these materials and the chemistries they catalyze.

## CONCLUSIONS

Framework Sn sites in siliceous Beta zeolites exhibit unique adsorption properties that differ from those observed with nonframework SnO<sub>2</sub>. For acetonitrile, diethyl ether, and 2-methyl-2-propanol, adsorption complexes with nearly one molecule per Sn site stoichiometry have been identified. Characterization of these adsorption complexes provides a convenient method for understanding the catalytic properties of the materials. In particular, FTIR spectra of acetonitrile-*d*<sub>3</sub> provide a convenient method for characterizing the presence of framework Sn sites.

## ASSOCIATED CONTENT

### Supporting Information

Further details are given in Figures S1–S4. This material is available free of charge via the Internet at <http://pubs.acs.org>.

## AUTHOR INFORMATION

### Corresponding Author

\*Phone: +1 215 898 4439. Fax: +1 215 573 2093. E-mail: [gorte@seas.upenn.edu](mailto:gorte@seas.upenn.edu).

### Present Address

<sup>§</sup>Department of Chemistry, BITS Pilani, Hyderabad Campus, Shameerpet, Hyderabad, India.

### Notes

The authors declare no competing financial interest.

## ACKNOWLEDGMENTS

This work was supported as part of the Catalysis Center for Energy Innovation, an Energy Frontier Research Center funded by the U.S. Department of Energy, Office of Science, Office of Basic Energy Sciences under Award no. DE-SC0001004. We acknowledge Dr. S. Bai for collecting the solid state <sup>119</sup>Sn MAS NMR spectra.

## REFERENCES

- (1) Corma, A.; Nemeth, L. T.; Renz, M.; Valencia, S. *Nature* **2001**, *412*, 423–425.
- (2) Corma, A.; Domine, M. E.; Valencia, S. *J. Catal.* **2003**, *215*, 294–304.
- (3) Moliner, M.; Román-Leshkov, Y.; Davis, M. E. *Proc. Natl. Acad. Sci. U.S.A.* **2010**, *107*, 6164–6168.
- (4) Holm, M. S.; Pagán-Torres, Y. J.; Saravanamurugan, S.; Riisager, A.; Dumesic, J. A.; Taarning, E. *Green Chem.* **2012**, *14*, 702.
- (5) Newsam, J.; Tracey, M.; Koetsier, W.; De Guyter, C. *Proc. R. Soc. London A* **1988**, *420*, 375–405.
- (6) Boronat, M.; Concepcion, P.; Corma, A.; Renz, M.; Valencia, S. *J. Catal.* **2005**, *234*, 111–118.
- (7) Bordiga, S.; Bonino, F.; Damin, A.; Lamberti, C. *Phys. Chem. Chem. Phys.* **2007**, *9*, 4854–4878.
- (8) Gorte, R. J.; White, D. *Top. Catal.* **1997**, *4*, 57.
- (9) Gorte, R. J. *Catal. Lett.* **1999**, *62*, 1.
- (10) Lee, C.-C.; Gorte, R. J.; Farneth, W. E. *J. Phys. Chem. B* **1997**, *101*, 3811.
- (11) Kresnawahjuesa, O.; Gorte, R. J.; White, D. *J. Mol. Catal. A* **2004**, *212*, 309.
- (12) Cambor, M. A.; Corma, A.; Valencia, S. *Chem. Commun.* **1996**, 2365.
- (13) Xu, X.; Wang, J.; Long, Y. *Chin. J. Chem.* **2006**, *24*, 1725–1730.
- (14) Bermejo-Deval, R.; Gounder, R.; Davis, M. E. *ACS Catal.* **2012**, *2* (12), 2705–2713.
- (15) Jentoft, F. C. *Adv. Catal.* **2009**, *52*, 129–211.
- (16) Holland, T.; Redfern, S. *Mineral. Mag.* **1997**, *61*, 65–77.
- (17) Roy, S.; Bourbakis, G.; Hong, D.-Y.; Vlachos, D.; Bhan, A.; Gorte, R. J. *ACS Catal.* **2012**, *2*, 1846.
- (18) Bermejo-Deval, R.; Assary, R. S.; Nikolla, E.; Moliner, M.; Roman-Leshkov, Y.; Hwang, S. J.; Palsdottir, A.; Silverman, D.; Lobo, R. F.; Curtiss, L. A.; Davis, M. E. *Proc. Natl. Acad. Sci. U.S.A.* **2012**, *109* (25), 9727–9732.
- (19) Weber, R. J. *Catal.* **1995**, *151*, 470–474.
- (20) Pang, G.; Chen, S.; Koltypin, Y.; Zaban, A.; Feng, S.; Gedanken, A. *Nano Lett.* **2001**, *1*, 723–726.
- (21) Chezeau, J. M.; Delmotte, L.; Guth, J. L.; Gabelica, Z. *Zeolites* **1991**, *6*, 598.
- (22) Savitz, S.; Myers, A. L.; Gorte, R. J. *Microporous Mesoporous Mater.* **2000**, *37*, 33.
- (23) Kotrla, J.; Kubelkova, L.; Lee, C.-C.; Gorte, R. J. *J. Phys. Chem. B* **1998**, *102*, 1437.



- (24) Barthel, J.; Deser, R. J. *Solution Chem.* **1994**, *23*, 1133.
- (25) Roman-Leshkov, Y.; Moliner, M.; Labinger, J. A.; Davis, M. E. *Angew. Chem., Int. Ed.* **2010**, *49* (47), 8954–8957.
- (26) Demmin, R. A.; Gorte, R. J. *J. Catal.* **1984**, *90*, 32.